

The saturated ion current  $I_s$  collected by the probe is given by

$$I_s = \frac{1}{4} n_{i_s} e A_p \bar{c}_{i_s}, \quad (7)$$

where  $n_{i_s}$  is the ion density at the sheath edge,  $A_p$  the probe collection area,  $e$  the unit charge, and  $\bar{c}_{i_s} = (8kT_s/\pi m_i)^{1/2}$  the ion random thermal velocity at the sheath edge. If the sheath edge (which can be calculated in the way described in the original paper<sup>1</sup>) falls within the region of constant ion density in the boundary layer, then an increase in probe-plasma potential difference at the ion saturation limit will produce an increase in the saturation ion current only through the change in  $T_s^{1/2}$  with sheath thickness, since the sheath grows outward with essentially constant area in a constant ion density region. Consequently, in such cases one expects the stagnation-point probe characteristic curve to exhibit a more constant ion saturation current limit than is obtained with cylindrical or spherical probes, and this has in fact been observed in experiments carried out at Berkeley. It is interesting to observe that if  $Le = 1$ , Eq. (7) takes on the particularly simple form

$$n_{i_s} = (2\pi m_i/kT_s)^{1/2} (I_s/eA_p) \quad (8)$$

in which the only quantity not directly measured is the ion temperature  $T_s$  at the sheath edge, and this temperature may be calculated by the method already described.<sup>1</sup> The free-stream ion density is given by  $n_{i_s} = \epsilon n_{i_\infty}$ , where  $\epsilon = \rho_1/\rho_2$  is the density ratio across the shock wave.

All of the preceding analysis is applicable as well to a double-probe<sup>2</sup> configuration at the stagnation point, where one of the probe elements is at the ion-saturation limit. The advantages of the double probe over the single probe are that the current drain from the plasma never exceeds the ion saturation current, and that the electron temperature is usually more easily determined from the symmetric double-probe characteristic curve than from the single-probe characteristic. Two convenient double-probe configurations which have been used at Berkeley<sup>3</sup> are sketched in Fig. 1. These configurations have the property that the two collection elements "see" identical flow regions in the stagnation-point boundary layer, if the flow is axisymmetric. A concentric ring geometry, such as was

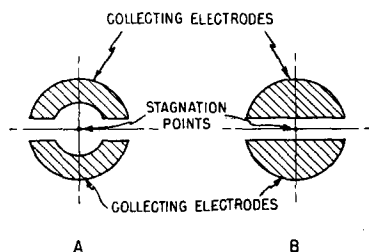


FIG. 1. Two configurations for the stagnation-point double probe.

mentioned earlier,<sup>1</sup> does not possess this property.

In conclusion, I wish to correct several errors which appeared in the original paper.<sup>1</sup> First, Eq. (12) should read  $D_a = (\bar{\mu}_i D_e + \bar{\mu}_e D_i)/(\bar{\mu}_i + \bar{\mu}_e)$ . Also, the expression for  $\bar{c}(\eta_i)$ , which has the same meaning as  $\bar{c}_{i_s}$ , is incorrectly written in the Example, and should read as given below Eq. (7) of this note. Attention is called to another misprint, in Eq. (22), which should read

$$v = -\frac{1}{\rho r_0} \left[ \frac{f}{(2s)^{1/2}} \frac{ds}{dx} + (2s)^{1/2} \frac{\partial \eta}{\partial x} \right].$$

Finally, in the Example the free-stream ion density was computed incorrectly, since the factor  $n_o/n_e$  was omitted in the expression for  $z$  (see second paragraph of present note). The inclusion of this factor changes some of the numerical results which follow. Corrected values are  $n_{i_s} = 2.9 \times 10^{17}/\text{m}^3$ ,  $n_{i_\infty} = 0.9 \times 10^{17}/\text{m}^3$ . Certain other numerical results should be changed accordingly, but since the Example was only hypothetical, it does not seem necessary to detail these numerical changes.

This work was supported by the Air Force Office of Scientific Research under contract AF 49(638)-502.

<sup>1</sup> L. Talbot, *Phys. Fluids* **3**, 289 (1960). The notation of the present note conforms to that of this paper, unless otherwise noted.

<sup>2</sup> E. O. Johnson and L. Malter, *Phys. Rev.* **89**, 58 (1950).

<sup>3</sup> F. S. Sherman and L. Talbot in *Progress in Astronautics and Rocketry* (Academic Press Inc., New York, 1962), Vol. 7, p. 581.

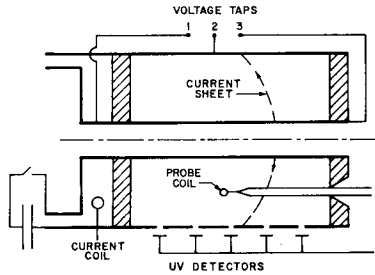
## Current Distribution in a Magnetic Annular Shock Tube

JAMES C. KECK

Avco-Everett Research Laboratory, Everett, Massachusetts  
(Received January 22, 1962)

THE magnetic annular shock tube<sup>1</sup> is among the most promising devices for producing high-velocity plasmas, and considerable research has been devoted to developing it both as a space propulsion device and as an injector for fusion reactors. Nevertheless, very little is known about the exact mechanism by which the magnetic field accelerates the gas. In particular, for a shock tube of large radius ratio, the magnetic pressure  $B^2/8\pi$  may decrease by orders of magnitude across the annulus and, thus, cannot be balanced by the constant dynamic pressure  $\rho u_s^2$  associated with a plane normal shock propagating ahead of it.<sup>2</sup> It is the purpose of this note to give a preliminary report of some studies of the shock shape and current distribution in a magnetic annular shock tube which may assist in achieving an understanding of the above question, as well as others involving the

FIG. 1. Schematic diagram of the magnetic-annular-shock-tube geometry.



dynamic interaction of a gas and a magnetic field. A schematic diagram of the apparatus used in the experiments is shown in Fig. 1. The electrodes of the magnetic annular shock tube were copper cylinders 36 in. long with inner and outer radii of 1 and 3 in. The insulators at the ends of the test section were lucite. The 378- $\mu$ f capacitor bank was connected to produce a current pulse rising in 2  $\mu$ sec to a value which remained constant for a test time of 12  $\mu$ sec. For the experiments reported here, the capacitor bank was charged to 5 kv which produced a peak current of 165 ka in argon at a pressure of 50  $\mu$  Hg. The back emf  $V_{13}$  was 1200 v and the arc drop  $V_{23}$  was approximately 50 v. We should note that no external fields or preionization were used in the present experiments.

The shock speed was measured by five tungsten uv detectors<sup>3</sup> spaced 6 in. apart along the length of the tube. For given operating conditions the shock speeds were reproducible and constant to  $\pm 3\%$  over the entire 24-in. interval spanned by the uv detectors. However, an unexpected dependence of the speed on the polarity of the center electrode was observed. The average speeds for positive and negative polarity were 5.3 and 4.7 cm/ $\mu$ sec, respectively.

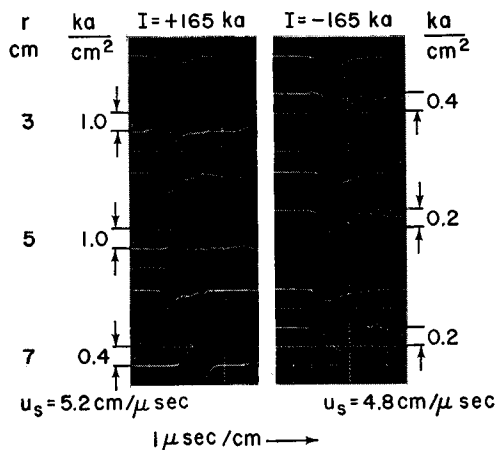


FIG. 2. Oscillograms of current density at the center of the annulus at an axial station 60 cm from the driver end for various radial positions and positive and negative center electrode. The lower trace in each oscillogram is the current density; the upper trace is a reference uv signal obtained from a detector looking across the annulus at the coil position.

The coils used to probe the magnetic field were constructed of a single turn of 5-mil Nyclad wire mounted on a glass sting. The design was based on the theory that if the diameter of the wire were made small compared to a mean free path, the interaction with the gas could be made negligible.

In the present experiment, the magnetic field in the shock tube was mapped out point by point, by inserting the probes as indicated in Fig. 1 to axial positions opposite the uv speed detectors and scanning radially in 1-cm steps across the 5-cm gap. Some typical oscillograms of the coil output voltage  $V_c$  are shown in Fig. 2. If we assume (as indicated by experiment) that the magnetic field is nearly steady in a coordinate frame moving at the shock speed, then  $V_c \approx 4\pi \times 10^{-9} A u_s j_r v$ , where  $u_s$  is

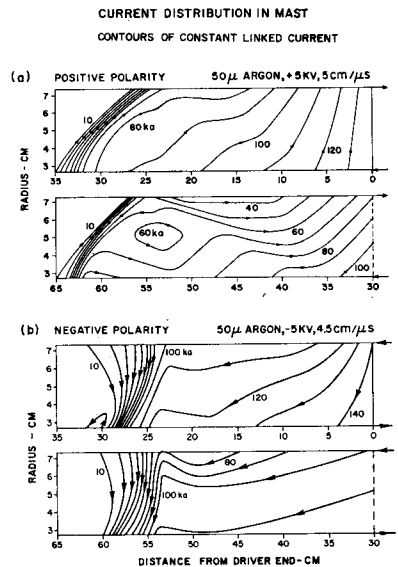


FIG. 3. Contour plots showing current distribution for positive and negative center electrode. Note that the axial scale of the figure has been compressed by a factor of 2.

the shock speed in cm/sec,  $A$  is the area of the coil in  $\text{cm}^2$ , and  $j_r$  is the radial current density in  $\text{amp}/\text{cm}^2$ . This equation was used to establish the calibration of the traces in Fig. 2.

It is immediately apparent from an inspection of Fig. 2 that the current pattern in the magnetic annular shock tube depends on the polarity of operation. For a positive (outward) radial current, the thickness of the current sheet is  $\sim 2$  cm, while for a negative (inward) current, it is more than twice as thick. Also, as can be seen by comparing the position of the current pulse with the reference signal from the uv detectors, the shape of the current sheet changes when the polarity of operation is reversed. For positive operation, the current sheet is severely canted with the inner edge leading the outer edge by 1.5  $\mu$ sec in time or 8 cm in space. For negative operation the sheet, although not as well defined, is more or less perpendicular to the walls.

A more quantitative picture of the current distribution is given in Fig. 3. Here we show contours of constant linked current  $I = 5 B_0 r$  obtained by RC integration of the signals in Fig. 2 at two instants in time for both positive and negative operation. All the features of the leading current sheet mentioned above are clearly seen in Fig. 3. An important feature not shown is that there exists a  $B_0$  ahead of the current sheet even though none was applied. This  $B_0$  has a value of almost exactly 1/10 the initial field jump and is associated with an approximately constant current per unit electrode length established in the first fraction of a microsecond after initiation of the discharge during which time the conductivity of the gas is presumably rising to a high enough value to exclude the field.

The development of the current pattern behind the current sheet can also be seen in Fig. 3. For the case of positive operation, the current distribution suggests the growth of a gas "bubble" on the outside wall behind the current sheet. (In this connection, note that the direction of the magnetic pressure is down the gradient of the contours.) For the case of negative operation most of the drive current flows at the shock front. A tentative explanation of the observations presented here is given in the following Note.

This work is supported by Air Force Office of Scientific Research, Air Research and Development Command, United States Air Force, under Contract AF 49(638)-659.

<sup>1</sup> G. S. Janes and R. M. Patrick, in *Conference on Extreme High Temperatures*, edited by H. Fischer and L. Mansur (John Wiley & Sons, Inc., New York, 1958).

<sup>2</sup> J. C. Keck, F. Fishman, and H. E. Petschek, *Bull. Am. Phys. Soc.* **6**, 278 (1961).

<sup>3</sup> M. Camac, A. R. Kantrowitz, M. M. Litvak, R. M. Patrick, and H. E. Petschek, Paper presented at the International Atomic Energy Agency Meeting, Salzburg, Austria (1961).

## Flow Model for Large Radius-Ratio Magnetic Annular Shock-Tube Operation

F. J. FISHMAN AND H. PETSCHKEK  
Avco-Everett Research Laboratory, Everett, Massachusetts  
(Received January 22, 1962)

IN this note we propose a model that explains some features of the behavior of magnetic annular shock tubes of large radius ratio as reported by Keck in the preceding note. Topics discussed are the shape of the current sheet when the center electrode is positive, the speed of this current sheet, and the difference between positive and negative operation.

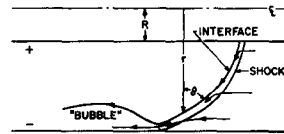


FIG. 1. Flow model for large annulus ratio.

We first consider a model based on the assumptions: (1) the gas is sufficiently conducting so that the magnetic field does not penetrate into the plasma, i.e., the current is confined to a thin sheet forming the boundary between gas and field; (2) the current flows freely from plasma to electrodes. The total pressure must be continuous across a current sheet, hence, the gas pressure on one side balances the magnetic pressure on the other side. Now the magnetic field varies inversely with radius, so that the magnetic pressure at the inside cylinder greatly exceeds that at the outside. This suggests that the current sheet at the inside is pushed ahead relative to the outside. The model sketched in Fig. 1 is proposed. The current sheet may be regarded as a solid body moving through the gas. A shock wave will form slightly ahead of the current sheet; this shock deflects the flow so that it goes around the current sheet. When this flow reaches the outside wall, its radial motion is stopped and therefore its pressure increased, moving the current sheet further away from the wall and allowing the gas to flow through and form a bubble.

In a coordinate system moving with the current sheet, the forward part of this sheet would be expected to be a steady flow, although the bubble will grow in time. The shape of the steady portion may be computed from the pressure balance condition. In hypersonic flow with a thin shocked layer (as assumed above) the gas pressure at the sheet is approximately the normal component of the momentum flux ahead of the shock,<sup>1</sup> i.e.,

$$p = \rho_1 u_s^2 \cos^2 \theta, \quad (1)$$

where  $\rho_1$  is the gas density ahead of the shock,  $u_s$  is the flow velocity (i.e., the sheet speed in laboratory coordinates), and  $\theta$  is angle between the flow velocity and the normal to the sheet. The pressure balance condition becomes

$$\rho_1 u_s^2 \cos^2 \theta = (B_0^2/8\pi)(R/r)^2 \quad (2)$$

with  $B_0$  the magnetic field at the inner radius  $R$ , and  $r$  the local radius. We assume that at  $R$  the current sheet forms a right angle with the inside wall. This follows from Eq. (1) if one assumes that at a corner of arbitrary angle the full stagnation pressure  $\rho_1 u_s^2$ , would be developed. This boundary condition and Eq. (2) determine the sheet propagation speed to be

$$u_s = B_0(8\pi\rho_1)^{-1/2}. \quad (3)$$